

# A Modified Sparsified Nested Dissection Ordering Preconditioner for Discrete Exterior Calculus Solver Using Vector-Scalar Potentials

Boyuan Zhang and Weng Cho Chew\*

*Elmore Family School of Electrical and Computer Engineering, Purdue University, West Lafayette, IN 47907, USA*

**ABSTRACT:** A broadband preconditioner based on a modified version of the sparsified nested dissection ordering (m-spaNDO) technique is proposed for the full wave discrete exterior calculus (DEC)  $\mathbf{A}-\Phi$  formulation solver in electromagnetics. The matrix equation discretized by the DEC  $\mathbf{A}-\Phi$  solver is in general complex symmetric and indefinite. When conductive media and disparate mesh are involved, the DEC  $\mathbf{A}-\Phi$  matrix equation is ill-conditioned, and proper preconditioner must be utilized to accelerate iterative solver convergence. In this letter, an introduction to the DEC  $\mathbf{A}-\Phi$  solver is provided, followed by the implementation details of the m-spaNDO preconditioner. Numerical examples in this paper show that the proposed m-spaNDO preconditioner can effectively accelerate the convergence of iterative solvers in solving ill-conditioned problems. The m-spaNDO preconditioned DEC  $\mathbf{A}-\Phi$  solver has  $O(N \log N)$  computational complexity and the efficiency of the preconditioner is independent of change in parameters such as frequency and conductivity in the problem, which indicates the broadband stable nature of the m-spaNDO preconditioner.

## 1. INTRODUCTION

The  $\mathbf{A}-\Phi$  formulation in electromagnetics is under active study [1–3], where  $\mathbf{A}$  and  $\Phi$  are the vector and scalar potential of the electromagnetic field, respectively. Compared with traditional  $\mathbf{E}-\mathbf{H}$  formulation, the  $\mathbf{A}-\Phi$  formulation is free of low-frequency breakdown, thanks to the additional gauge term that removes the null space of the double curl operator. Recently, a numerical  $\mathbf{A}-\Phi$  formulation solver based on discrete exterior calculus (DEC) is proposed, which showed its broadband stability from DC to optics [2]. Thus, the DEC  $\mathbf{A}-\Phi$  solver is ideal for broadband and multi-scale analysis, where static physics and wave physics could co-exist in the same problem and require the same solution accuracy. To make the DEC  $\mathbf{A}-\Phi$  solver capable of solving large scale problems, iterative solvers, such as the conjugate gradient (CG) method [4], biconjugate gradient (BiCG) method [5] and generalized minimal residual method (GMRES) [6], are preferred over direct solvers. This is because the error minimization mechanism in the iterative solvers allows user to control the effect of numerical error to the solution accuracy. However, when conductive media or disparate mesh in multi-scale structures are involved, the matrix equation discretized by the DEC  $\mathbf{A}-\Phi$  solver is ill-conditioned, and the iterative solvers converge very slowly or even fail to converge. In such cases, proper preconditioners are needed to accelerate the convergence of iterative solvers. Meanwhile, consider the broadband nature of the DEC  $\mathbf{A}-\Phi$  solver, the preconditioner should also be broadband in nature, i.e., its efficiency should be insensitive to change in parameters such as frequency and conductivity in the problem.

The construction of preconditioners is usually problem dependent. Due to the smoothness of the Green's function of electromagnetic wave equations [7], the coupling between separated structures is usually low-rank. In other words, in integral equation solvers, such as the method of moments (MoM), the resultant coupling matrix has low-rank off-diagonal mutual coupling blocks [8, 9]. One popular way to construct preconditioners is by compressing the low-rank off-diagonal matrix blocks, find the approximate inverse of the coupling matrix using fast arithmetics such as the hierarchical matrices ( $\mathcal{H}$ -matrices). The approximate inverse of the coupling matrix can be used as a preconditioner to the original matrix system. Depending on the compression technique utilized, such methods include the hierarchical off-diagonal low-rank (HODLR) format method [10], the hierarchically semiseparable (HSS) matrices [11] and the hierarchical interpolative factorization (HIF) method [12].

Different from the integral equation solver, where the discretized matrix is dense, the DEC  $\mathbf{A}-\Phi$  solver is a differential equation solver with sparse matrix system. However, by eliminating the interior unknowns in the computational domain, the remaining unknowns and their coupling are pushed to the boundary. The corresponding coupling matrix after interior unknown elimination is much denser, and shares similar physics with integral equation solver matrices [13]. In [9], a sparsified nested dissection ordering (spaNDO) algorithm is proposed as a preconditioner to the real symmetric positive definite matrix system discretized by differential equation solver, such as finite difference method (FDM) [14] and finite element method (FEM) [15].

\* Corresponding author: Weng Cho Chew (wcc@purdue.edu).

The sparsity pattern of the matrix equation discretized by differential equation solvers can be determined by the mesh information. Nested dissection ordering (NDO) algorithm takes advantage of the sparsity pattern information of the coupling matrix, creates separators in the computational domain and reorders the unknowns in the problem accordingly [16]. As a direct matrix equation solver, the computational complexity of NDO for factorizing the matrix system is  $O(N^2)$ , where  $N$  is the number of unknowns. In contrast, if one uses regular factorization method, such as the LU decomposition or the Gaussian elimination method, the computational complexity is  $O(N^3)$ . Although the  $O(N^2)$  complexity of NDO is proved to be the optimal complexity of direct solvers, it still makes the problem expensive when  $N$  gets large.

To further reduce the computational complexity, low-rank approximation can be introduced in NDO [9]. After the interior unknowns are eliminated, the remaining separator unknowns coupling is similar to an integral equation where the numerical Green's function is buried in the matrix. In electromagnetics, the coupling between separated objects is rank deficient [7, 8]. Thus, the off-diagonal mutual coupling blocks are low-rank and can be compressed to accelerate the computation of the approximate inverse of the coupling matrix. The spaNDO preconditioner in [9] effectively accelerates the convergence of iterative solvers in solving real symmetric positive definite matrix systems with  $O(N \log N)$  complexity. Such matrix systems are often encountered in mechanical systems. However, in computational electromagnetic (CEM) problems, when conductive medium is involved, the matrix system is not real-valued anymore. The DEC  $\mathbf{A}$ - $\Phi$  matrix system is in general complex symmetric and indefinite. Thus, the spaNDO preconditioner in [9] cannot be used directly to the DEC  $\mathbf{A}$ - $\Phi$  solver.

In this letter, a modified version of the spaNDO (m-spaNDO) is proposed, which works as an efficient preconditioner to the complex symmetric (non-Hermitian) matrix systems discretized by the DEC  $\mathbf{A}$ - $\Phi$  solver. The m-spaNDO preconditioner showed  $O(N \log N)$  computational complexity, and its efficiency is independent of frequency and conductivity parameters in the problems, which indicates its broadband property. The rest of the paper is organized as follows. In Section 2, introduction to the m-spaNDO preconditioned DEC  $\mathbf{A}$ - $\Phi$  solver is provided. In Section 3, numerical examples are presented to illustrate the complexity and broadband efficiency of the m-spaNDO preconditioner. In Section 4, discussion and conclusion of this letter are given.

## 2. THE m-spaNDO PRECONDITIONED DEC $\mathbf{A}$ - $\Phi$ SOLVER

### 2.1. The DEC $\mathbf{A}$ - $\Phi$ Solver

The  $\mathbf{A}$ - $\Phi$  formulation with generalized Lorenz gauge is [1]:

$$\nabla \times \frac{1}{\mu} \nabla \times \mathbf{A} - \omega^2 \tilde{\epsilon} \mathbf{A} - \tilde{\epsilon} \nabla [\chi^{-1} \nabla \cdot (\tilde{\epsilon} \mathbf{A})] = \mathbf{J}_{im}, \quad (1)$$

$$\nabla \cdot (\tilde{\epsilon} \nabla \Phi) + \omega^2 \chi \Phi = -\rho_{im}, \quad (2)$$

where  $\mathbf{A}$  and  $\Phi$  are the vector and scalar potential of the electromagnetic field, respectively;  $\mathbf{J}_{im}$  and  $\rho_{im}$  are the impressed current density and impressed charge density, respectively;  $\omega$  is the angular frequency;  $\mu$  is the permeability;  $\tilde{\epsilon} = \epsilon + \frac{i\sigma}{\omega}$  is the complex permittivity;  $\epsilon$  and  $\sigma$  are the permittivity and conductivity, respectively;  $\chi = \alpha \mu \tilde{\epsilon}^2$  and  $\alpha$  is an arbitrary non-zero constant. The generalized Lorenz gauge is used to decouple the  $\mathbf{A}$  and  $\Phi$  equations [1]:

$$\nabla \cdot (\tilde{\epsilon} \mathbf{A}) = i\omega \chi \Phi. \quad (3)$$

Eqs. (1) and (2) can be discretized by using DEC [2, 17, 18] with tetrahedral mesh, which generates the matrix equations:

$$\begin{aligned} & \left( \bar{\mathbf{d}}^{(1)} \right)^T \star_{\mu^{-1}}^{(2)} \bar{\mathbf{d}}^{(1)} \mathbf{A} - \omega^2 \star_{\epsilon}^{(1)} \mathbf{A} \\ & + \star_{\epsilon}^{(1)} \bar{\mathbf{d}}^{(0)} \star_{\chi^{-1}}^{(3)} \left( \bar{\mathbf{d}}^{(0)} \right)^T \star_{\epsilon}^{(1)} \mathbf{A} = \mathbf{J}, \end{aligned} \quad (4)$$

$$- \left( \bar{\mathbf{d}}^{(0)} \right)^T \star_{\epsilon}^{(1)} \bar{\mathbf{d}}^{(0)} \Phi + \omega^2 \star_{\chi}^{(0)} \Phi = -\rho. \quad (5)$$

where  $\mathbf{A} = [A_1, A_2, \dots, A_{N_1}]^T$  is the vector that contains the vector potential unknowns  $A_i$  on each edge in the mesh;  $\Phi = [\Phi_1, \Phi_2, \dots, \Phi_{N_0}]^T$  is the vector that contains the scalar potential unknowns  $\Phi_i$  on each node in the mesh;  $N_1$  and  $N_0$  are the total number of edges and nodes in the mesh.

Matrices  $\bar{\mathbf{d}}^{(0)}$  and  $\bar{\mathbf{d}}^{(1)}$  are called incidence matrices which are the discrete representations of the gradient and curl operators on the primal mesh, respectively. They can be constructed by using the connectivity information in the mesh.

$\star_{\epsilon}^{(1)}$ ,  $\star_{\mu^{-1}}^{(2)}$  and  $\star_{\chi}^{(0)}$  are the Galerkin Hodge star operators representing the constitutive relations. For simplicity of this letter, the details are omitted but can be found in [2].

### 2.2. Nested Dissection Ordering in DEC $\mathbf{A}$ - $\Phi$ Solver

In this section, (4) is used as an example to demonstrate how to construct its m-spaNDO preconditioner. (4) can be written compactly as:

$$\bar{\mathbf{M}} \mathbf{A} = \mathbf{J}, \quad (6)$$

where  $\bar{\mathbf{M}}$  is the coupling matrix among the unknowns in  $\mathbf{A}$ . The sparsity pattern of  $\bar{\mathbf{M}}$  can be determined from the mesh connectivity information. By using NDO, separators are constructed in the computational domain, and unknowns are reordered accordingly. A separator in NDO is comprised of a set of unknowns. By removing the edges associated with the separator unknowns from the mesh, the remaining unknowns form two clusters that are decoupled from each other [9, 16]. Fig. 1 shows an example of NDO separator in 2D case, where the unknown set  $\mathbf{A}_3$  is the separator,  $\mathbf{A}_1$  and  $\mathbf{A}_2$  are two decoupled unknown clusters that are separated by  $\mathbf{A}_3$ . Accordingly, the unknowns in vector  $\mathbf{A}$  in (6) are reordered as:

$$\mathbf{A} = [\mathbf{A}_1, \mathbf{A}_2, \mathbf{A}_3]^T. \quad (7)$$

Since  $\mathbf{A}_1$  and  $\mathbf{A}_2$  are decoupled,  $\bar{\mathbf{M}}$  has the following structure:

$$\bar{\mathbf{M}} = \begin{bmatrix} \bar{\mathbf{M}}_{11} & \mathbf{0} & \bar{\mathbf{M}}_{13} \\ \mathbf{0} & \bar{\mathbf{M}}_{22} & \bar{\mathbf{M}}_{23} \\ \bar{\mathbf{M}}_{31} & \bar{\mathbf{M}}_{32} & \bar{\mathbf{M}}_{33} \end{bmatrix}, \quad (8)$$

where  $\bar{\mathbf{M}}_{ii}$  is the self-coupling matrix among unknowns in  $\mathbf{A}_i$ , and the off-diagonal blocks represent the mutual couplings. Unknown sets  $\mathbf{A}_1$ ,  $\mathbf{A}_2$  and  $\mathbf{A}_3$  are eliminated successively in a divide-and-conquer (DaD) fashion, which introduces minimum matrix element fill-ins in the elimination procedure [9]. This is the key reason that NDO can achieve the optimal  $O(N^2)$  complexity as a direct solver.

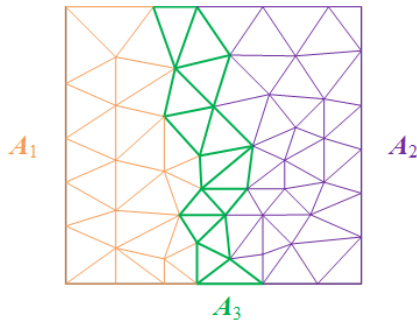


FIGURE 1. The construction of a NDO separator in 2D case.

Different levels of separators in NDO can be constructed recursively. Fig. 2 illustrates the procedure of constructing two levels of separators in 2D case. After the top level separator is constructed in Fig. 2(b), two  $l = 2$  level separators are further constructed in each of the subregions in Fig. 2(c).

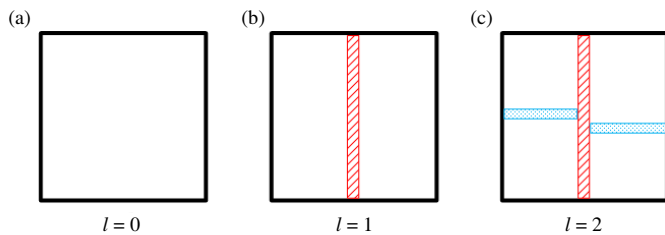


FIGURE 2. An example of constructing different levels of separators in 2D case. (a) The original computational domain. (b) The  $l = 1$  level separator. (c) The  $l = 2$  level separators.

Accordingly, Fig. 3 shows the elimination tree associated with the NDO separator in Fig. 2(c). There are four leaf-level unknown clusters, which correspond to the four ‘white spaces’ in Fig. 2(c). The three circle nodes in the elimination tree correspond to the three separators in Fig. 2(c).

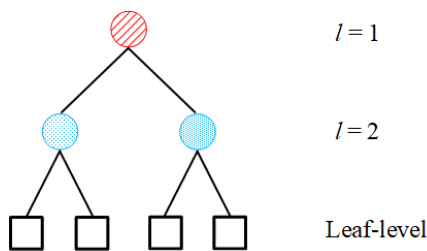


FIGURE 3. The elimination tree associated with the NDO separator in Fig. 2(c).

After the unknowns in  $\mathbf{A}$  in (6) are reordered following the NDO separation, elimination of unknowns should be performed from bottom level to top level in the elimination tree, i.e., from leaf-level clusters to the top level separator cluster [9, 16].

### 2.3. The Modified Version of spaNDO Preconditioner

After the elimination of the leaf-level unknown clusters, (6) becomes

$$\bar{\mathbf{M}}_s \mathbf{A}_s = \mathbf{J}_s, \quad (9)$$

where  $\mathbf{A}_s$  only contains the separator unknowns, and  $\bar{\mathbf{M}}_s$  is a dense matrix that represents the couplings among the separator unknowns. Note that  $\bar{\mathbf{M}}_s$  has similar physics as the matrix discretized by integral equation solvers. Thus, the off-diagonal blocks in  $\bar{\mathbf{M}}_s$ , which represent the mutual couplings of the separator clusters, are low-rank. By exploiting the low-rank nature of the off-diagonal blocks, the approximate inverse of  $\bar{\mathbf{M}}_s$  can be computed with much cheaper computational cost.

When eliminating a certain separator cluster  $\mathbf{A}_a$ , one can consider the following frontal matrix extracted from  $\bar{\mathbf{M}}_s$ :

$$\tilde{\mathbf{M}} = \begin{bmatrix} \bar{\mathbf{M}}_{aa} & \bar{\mathbf{M}}_{ab} \\ \bar{\mathbf{M}}_{ba} & \bar{\mathbf{M}}_{bb} \end{bmatrix}, \quad (10)$$

where  $\bar{\mathbf{M}}_{aa}$  is the self-coupling matrix among the unknowns in separator  $\mathbf{A}_a$ ;  $\mathbf{A}_b$  denotes all the unknowns in other separators that couple to  $\mathbf{A}_a$ . The meaning for  $\bar{\mathbf{M}}_{ab}$ ,  $\bar{\mathbf{M}}_{ba}$  and  $\bar{\mathbf{M}}_{bb}$  are self-explained.

Since  $\bar{\mathbf{M}}_{ab}$  and  $\bar{\mathbf{M}}_{ba}$  are low-rank, the following procedure can be performed as the sparsified nested dissection ordering. First, a scaling step with respect to  $\bar{\mathbf{M}}_{aa}$ :

$$\tilde{\mathbf{M}} \rightarrow \begin{bmatrix} \bar{\mathbf{I}} & \bar{\mathbf{L}}^{-1} \bar{\mathbf{M}}_{ab} \\ \bar{\mathbf{M}}_{ba} \bar{\mathbf{U}}^{-1} & \bar{\mathbf{M}}_{bb} \end{bmatrix} = \begin{bmatrix} \bar{\mathbf{I}} & \bar{\mathbf{C}}_{ab} \\ \bar{\mathbf{C}}_{ba} & \bar{\mathbf{M}}_{bb} \end{bmatrix} = \tilde{\mathbf{M}}_1, \quad (11)$$

where the LU decomposition,  $\bar{\mathbf{M}}_{aa} = \bar{\mathbf{L}}\bar{\mathbf{U}}$ , is involved in the above operation.

Second, one can perform methods such as singular value decomposition (SVD) [19], randomized SVD [20], or rank-revealing QR factorization [21] to  $\bar{\mathbf{C}}_{ab}$  and  $\bar{\mathbf{C}}_{ba}$  to explore their low-rank property. Eventually,  $\tilde{\mathbf{M}}_1$  in (11) can be transformed into

$$\tilde{\mathbf{M}}_1 \rightarrow \begin{bmatrix} \bar{\mathbf{I}}_{ff} & \mathbf{0} & \bar{\mathbf{W}}_f \\ \mathbf{0} & \bar{\mathbf{I}}_{cc} & \bar{\mathbf{W}}_c \\ \bar{\mathbf{N}}_f & \bar{\mathbf{N}}_c & \bar{\mathbf{M}}_{bb} \end{bmatrix} \approx \begin{bmatrix} \bar{\mathbf{I}}_{ff} & \mathbf{0} & \mathbf{0} \\ \mathbf{0} & \bar{\mathbf{I}}_{cc} & \bar{\mathbf{W}}_c \\ \mathbf{0} & \bar{\mathbf{N}}_c & \bar{\mathbf{M}}_{bb} \end{bmatrix} = \tilde{\mathbf{M}}_2. \quad (12)$$

In the above, it is assumed that  $\mathbf{A}_a = [\mathbf{A}_f, \mathbf{A}_c]^T$ , where the subscripts  $f$  and  $c$  stand for *fine* and *coarse*, respectively, following the terminology from [9]. The fine unknowns, whose self-coupling matrix is  $\bar{\mathbf{I}}_{ff}$  in (12), represent the redundant mutual couplings among separators. Specifically, in (12),  $\|\bar{\mathbf{W}}_f\|_{\text{row}} < \xi \|\bar{\mathbf{W}}_c\|_{\text{row}}$  and  $\|\bar{\mathbf{N}}_f\|_{\text{col}} < \xi \|\bar{\mathbf{N}}_c\|_{\text{col}}$ , where  $\|\cdot\|_{\text{row}}$  and  $\|\cdot\|_{\text{col}}$  denote the maximum row norm and the maximum column norm of a matrix, respectively;  $\xi$  is the prescribed tolerance chosen for the low-rank approximation (LRA).

Apparently, the fine unknowns  $\mathbf{A}_f$  are approximately eliminated without introducing any element fill-ins to  $\bar{\mathbf{M}}_{bb}$  in (12). This sparsification step can be performed with respect to each separator before eliminating a certain level of separators. It is

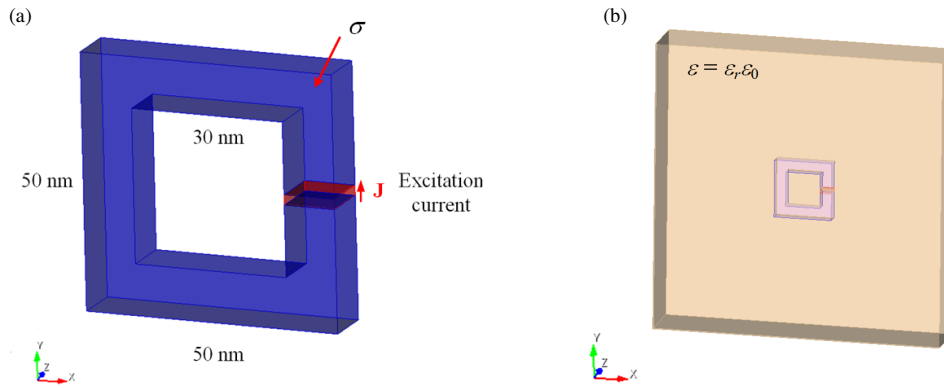


FIGURE 4. (a) Dimension of the rectangular wire loop and (b) the wire loop is placed in dielectric region.

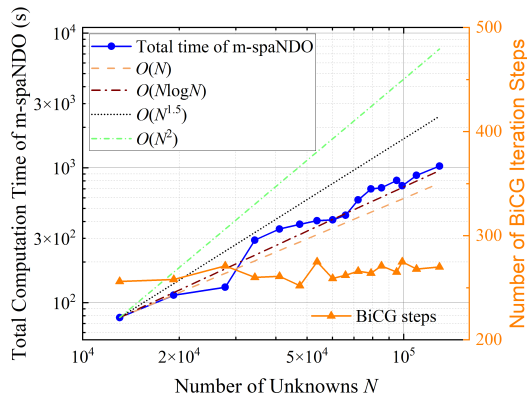


FIGURE 5. Summary of the total computation time and BiCG iteration steps of the proposed m-spaNDO preconditioned DEC  $\mathbf{A}-\Phi$  solver.

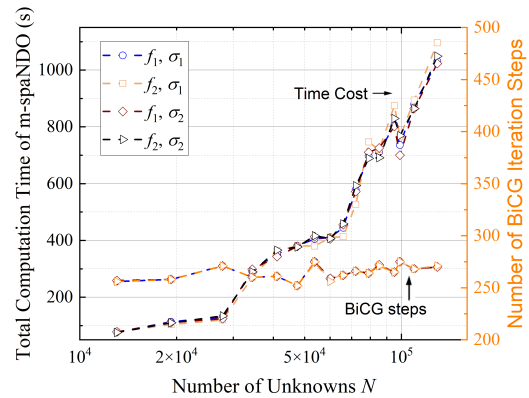


FIGURE 6. Study on the efficiency of the m-spaNDO preconditioned DEC  $\mathbf{A}-\Phi$  solver with different frequencies and conductivities.

equivalent to reducing the number of unknowns in each separator with very small computational cost. Thus, the computational complexity of the m-spaNDO is greatly reduced compared to that of NDO.

A theoretical analysis of the computational complexity of the original spaNDO preconditioner is carried out in [9]. As the m-spaNDO proposed in this letter shares the same basic steps compared to the spaNDO in [9], it also has  $O(N \log N)$  complexity.

### 3. NUMERICAL EXAMPLE

A rectangular wire loop case is used as a numerical example to validate the proposed m-spaNDO preconditioner. As shown in Fig. 4, the wire loop is assumed to be copper with conductivity  $\sigma = 5.8 \times 10^7$  S/m and is placed in air with  $\epsilon_r = 1$ . The frequency of the impressed current source is  $f = 1$  GHz. In this case, the complex permittivity  $\tilde{\epsilon}$  in the copper region is 9 orders larger than that in the air region. The coupling matrix  $\bar{\mathbf{M}}$  in (6) has humongous condition number due to the huge contrast in  $\tilde{\epsilon}$ . When using iterative solvers without preconditioning, it is extremely slow, sometimes even impossible, for the iterative solvers to converge.

As a contrast, the proposed m-spaNDO preconditioner is constructed with respect to the rectangular wire loop problem.

Biconjugate gradient (BiCG) method is used as the iterative solver. Fig. 5 summarizes the total computation time and BiCG iteration steps of the proposed m-spaNDO preconditioned DEC  $\mathbf{A}-\Phi$  solver with different numbers of unknowns  $N$ . Here, the total computation time includes the time cost in constructing the m-spaNDO preconditioner and the BiCG iteration procedure. The DEC  $\mathbf{A}-\Phi$  matrix equation set up time, which is linear with respect to  $N$  and is negligible compared to the solving time, is excluded from the total time.

As can be seen from Fig. 5, the total computation time of the m-spaNDO preconditioned DEC  $\mathbf{A}-\Phi$  solver fluctuates around  $O(N \log N)$  complexity. The reason for the fluctuation is that when conducting the theoretical complexity analysis of NDO and spaNDO,  $N$  is assumed to be a multiple of 2 [9]. To flatten the fluctuation, one can construct more than one separator in each subregion in Fig. 2, and accordingly, the elimination tree in Fig. 3 is not binary anymore.

The sensitivity of the m-spaNDO preconditioning efficiency to parameters such as frequency and conductivity in the problem is studied as well. Two frequencies are considered,  $f_1 = 1$  GHz and  $f_2 = 1$  kHz, along with two conductivities of the wire loop,  $\sigma_1 = 5.8 \times 10^7$  S/m and  $\sigma_2 = 5.8 \times 10^2$  S/m. Fig. 5 shows the total computation time of the m-spaNDO preconditioned solver and the BiCG iterations in different cases. The efficiency of the m-spaNDO preconditioned DEC  $\mathbf{A}-\Phi$  solver

is almost independent of the frequency and conductivity in the problem. This indicates the m-spaNDO preconditioner is stable and broadband.

#### 4. CONCLUSION

A modified version of the sparsified NDO (m-spaNDO) preconditioner is proposed. The m-spaNDO preconditioner works for the complex symmetric, indefinite matrix systems discretized from the DEC  $\mathbf{A}\text{-}\Phi$  solver. The m-spaNDO preconditioner effectively accelerates the convergence of iterative solvers in solving the DEC  $\mathbf{A}\text{-}\Phi$  matrix equations, especially when conductive media and disparate mesh are involved. The m-spaNDO preconditioned DEC  $\mathbf{A}\text{-}\Phi$  solver has  $O(N \log N)$  computational complexity, and its efficiency is independent of parameters such as frequency and conductivity in the problem. Thus, the proposed m-spaNDO preconditioner can work as an effective and broadband preconditioner for the DEC  $\mathbf{A}\text{-}\Phi$  solver.

#### ACKNOWLEDGEMENT

This work was supported by NSF Grant No. 2202389 and the Consortium on Electromagnetics Technologies at Purdue University (<https://engineering.purdue.edu/CEMT>).

#### REFERENCES

- [1] Chew, W. C., "Vector potential electromagnetics with generalized gauge for inhomogeneous media: Formulation," *Progress In Electromagnetics Research*, Vol. 149, 69–84, 2014.
- [2] Zhang, B., D.-Y. Na, D. Jiao, and W. C. Chew, "An  $\mathbf{A}\text{-}\Phi$  formulation solver in electromagnetics based on discrete exterior calculus," *IEEE Journal on Multiscale and Multiphysics Computational Techniques*, Vol. 8, 11–21, 2022.
- [3] Zhao, Y. and W. N. Fu, "A new stable full-wave Maxwell solver for all frequencies," *IEEE Transactions on Magnetics*, Vol. 53, No. 6, 1–4, 2017.
- [4] Hestenes, M. R. and E. Stiefel, "Methods of conjugate gradients for solving linear systems," *Journal of Research of the National Bureau of Standards*, Vol. 49, No. 6, 409–436, 1952.
- [5] Fletcher, R., "Conjugate gradient methods for indefinite systems," in *Numerical Analysis: Proceedings of the Dundee Conference on Numerical Analysis*, 73–89, Berlin, Heidelberg, 1976.
- [6] Saad, Y. and M. H. Schultz, "GMRES: A generalized minimal residual algorithm for solving nonsymmetric linear systems," *SIAM Journal on Scientific and Statistical Computing*, Vol. 7, No. 3, 856–869, 1986.
- [7] Chew, W. C., "Computational electromagnetics: The physics of smooth versus oscillatory fields," *Philosophical Transactions of the Royal Society of London. Series A: Mathematical, Physical and Engineering Sciences*, Vol. 362, No. 1816, 579–602, 2004.
- [8] Chai, W. and D. Jiao, "Theoretical study on the rank of integral operators for broadband electromagnetic modeling from static to electrodynamic frequencies," *IEEE Transactions on Components, Packaging and Manufacturing Technology*, Vol. 3, No. 12, 2113–2126, 2013.
- [9] Cambier, L., C. Chen, E. G. Boman, S. Rajamanickam, R. S. Tuminaro, and E. Darve, "An algebraic sparsified nested dissection algorithm using low-rank approximations," *SIAM Journal on Matrix Analysis and Applications*, Vol. 41, No. 2, 715–746, 2020.
- [10] Ambikasaran, S., "Fast algorithms for dense numerical linear algebra and applications," Ph.D. dissertation, Stanford University, Stanford, CA, 2013.
- [11] Chandrasekaran, S., P. Dewilde, M. Gu, T. Pals, X. Sun, A.-J. v. d. Veen, and D. White, "Some fast algorithms for sequentially semiseparable representations," *SIAM Journal on Matrix Analysis and Applications*, Vol. 27, No. 2, 341–364, 2005.
- [12] Ho, K. L. and L. Ying, "Hierarchical interpolative factorization for elliptic operators: Differential equations," *Communications on Pure and Applied Mathematics*, Vol. 69, No. 8, 1415–1451, 2016.
- [13] Chew, W. C. and C.-C. Lu, "The use of Huygens' equivalence principle for solving the volume integral equation of scattering," *IEEE Transactions on Antennas and Propagation*, Vol. 41, No. 7, 897–904, 1993.
- [14] Taflove, A., S. C. Hagness, and M. Picket-May, "Computational electromagnetics: The finite-difference time-domain method," *The Electrical Engineering Handbook*, Vol. 3, 629–670, 2005.
- [15] Jin, J.-M., *The Finite Element Method in Electromagnetics*, John Wiley & Sons, 2015.
- [16] George, A., "Nested dissection of a regular finite element mesh," *SIAM Journal on Numerical Analysis*, Vol. 10, No. 2, 345–363, 1973.
- [17] Deschamps, G. A., "Electromagnetics and differential forms," *Proceedings of the IEEE*, Vol. 69, No. 6, 676–696, 1981.
- [18] Desbrun, M., A. N. Hirani, M. Leok, and J. E. Marsden, "Discrete exterior calculus," *arXiv:math.DG/0508341*, 2005.
- [19] Klema, V. and A. Laub, "The singular value decomposition: Its computation and some applications," *IEEE Transactions on Automatic Control*, Vol. 25, No. 2, 164–176, 1980.
- [20] Halko, N., P.-G. Martinsson, and J. A. Tropp, "Finding structure with randomness: Probabilistic algorithms for constructing approximate matrix decompositions," *SIAM Review*, Vol. 53, No. 2, 217–288, 2011.
- [21] Chan, T. F., "Rank revealing QR factorizations," *Linear Algebra and Its Applications*, Vol. 88, 67–82, 1987.